Electronic Supplementary Information

Unsymmetric Ir(III) phosphorescent complexes with both 2-phenylpyridine(ppy)- and 2-vinylpyridine(vpy)-type ligands bearing functional groups and their optoelectronic properties

Siqi Liu,[a] Zhao Feng,[a] Hongyan Wang,[a] Huaiteng Hang,[a] Daokun Zhong,[a] Xiaolong Yang,[a] Yuanhui Sun,[a] Bochao Su,[a] Xianbin Xu,[b] Zhen Feng,[b] Guijiang Zhou,[a*] and Bo Jiao[c]

[a] *Engineering Research Center of Energy Storage Materials and Devices，Ministry of Education, School of Chemistry, State Key Laboratory for Mechanical Behavior of Materials, Xi'an Jiaotong University, Xi'an 710049, P. R. China.*

[b] *Shaanxi Lighte Optoelectronics Material Co., Ltd. Building 3, No. 99, Longfeng Road, High-tech Zone, Xi'an, Shaanxi 710065, P. R. China*

[c] *Key Laboratory for Physical Electronics and Devices of the Ministry of Education, Faculty of Electronic and Information Engineering, Xi'an Jiaotong University, Xi'an 710049, P. R. China.*

Corresponding author E-mail address: zhougj@mail.xjtu.edu.cn (G. J. Zhou)

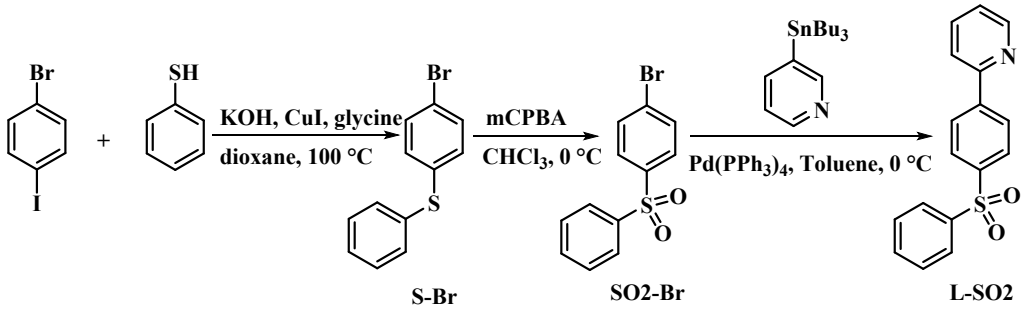

Scheme S1 Synthesis of the Key Intermediate Compounds L-SO2.

Synthesis of S-Br. Under nitrogen atmosphere, thiophenol (1.0 equiv), 1-Bromo-4-iodobenzene (1.0 equiv), KOH (2.5 equiv), CuI (0.05 equiv), glycine (0.2 equiv) and 1,4-dioxane (50 mL) were added and the reaction mixture was allowed to proceed at 100 ℃ for 16 h. After cooling to room temperature, the filter residue was filtered off and the filtrate was concentrated. The product was isolated with preparative thin-layer chromatography (TLC) on silica gel with petroleum ether as eluent.

Synthesis of SO2-Br. The reactant **S-Br** (1.0 equiv) was dissolved into $CHCl_3$ and then m-chloroperoxybenzoic acid (4.5 equiv) was slowly added under the condition of ice water bath. The mixture was stirred at room temperature for 72 h. The filtrate was concentrated after removing the filter residue and the crude product was purified by column chromatographed on silica gel using CH_2Cl_2 and petroleum ether (1:1, v/v) as eluent.

Synthesis of L-SO2. Under a N_2 atmosphere, **SO2-Br** (1.0 equiv), tributylpyridyltin (1.1 equiv) and catalyst $Pd(PPh_3)_4$ (0.05 equiv) were added and the mixture was heated to 110 ℃ for 16 h. After the reaction system was cooled to RT, the reaction mixture was concentrated and the crude product was separated and purified by silica gel column chromatography using CH_2Cl_2 and petroleum ether (2:1, v/v) as eluent.

L-SO2: yield 75 %. ^{1}H NMR (400 MHz, $CDCl_3$): δ (ppm) 8.71 (d, J = 4.8 Hz, 1 H), 8.13 (d, J = 8.4 Hz, 2 H), 8.04 (d, J = 8.8 Hz, 2 H), 7.97 (d, J = 7.2 Hz, 2 H), 7.81 – 7.74 (m, 2 H), 7.59 – 7.49 (m,

3 H), 7.32 – 7.29 (m, 1 H); ^{13}C NMR (100 MHz, $CDCl_3$): δ (ppm) 155.28, 149.99, 143.97, 141.55, 141.49, 137.02, 133.21, 129.28, 128.14, 127.71, 127.61, 123.26, 121.05.

General Procedure for Synthesis of L-1, L-2 and L-3. 2-Vinylpyridine (1.1 equiv), halogenated compounds (1.0 equiv) and catalyst $(PPh_3)_2PdCl_2$ (0.1 equiv) were added into triethylamine (20 mL) to obtain reaction mixture which was stirred for 16-19 h at 100 ℃. After cooling to room temperature, the solvent was removed and the crude product was purified on silica gel using the mixed solution of petroleum ether, CH_2Cl_2 and diethylene glycol monoether as eluent.

L-1: yield 65 %. ^{1}H NMR (400 MHz, $CDCl_3$): δ (ppm) 8.61 (d, *J* = 4.4 Hz, 1 H), 7.68 – 7.62 (m, 2 H), 7.59 (d, *J* = 7.6 Hz, 2 H), 7.40 – 7.38 (m, 3 H), 7.30 (t, *J* = 7.6 Hz, 1 H), 7.20 – 7.12 (m, 2 H); ^{13}C NMR (100 MHz, $CDCl_3$): δ (ppm) 155.53, 149.62, 136.57, 136.50, 132.63, 128.67, 128.28, 127.87, 127.05, 122.07, 122.02.

L-2: yield 44%. ^{1}H NMR (400 MHz, $CDCl_3$): δ (ppm) 8.59 (d, *J* = 4.0 Hz, 1 H), 7.63 (td, *J* = 2.0, 7.6 Hz, 1 H), 7.58 (d, *J* = 16.4 Hz, 1 H), 7.45 (d, *J* = 8.8 Hz, 2 H), 7.35 (d, *J* = 7.6 Hz, 1 H), 7.27 (t, *J* = 8.0 Hz, 4 H), 7.14 – 7.03 (m, 10 H); ^{13}C NMR (100 MHz, $CDCl_3$): δ (ppm) 155.89, 149.58, 147.97, 147.34, 136.43, 132.14, 130.42, 129.29, 127.97, 125.99, 124.72, 123.23, 122.96, 121.78, 121.63.

L-3: yield 65 %. ^{1}H NMR (400 MHz, $CDCl_3$): δ (ppm) 8.60 (d, *J* = 4.4 Hz, 1 H), 7.67 – 7.59 (m, 2 H), 7.56 – 7.54 (m, 2 H), 7.38 – 7.34 (m, 3 H), 7.15 – 7.01 (m, 7 H); ^{13}C NMR (100 MHz, $CDCl_3$): δ (ppm) 157.58, 156.72, 155.63, 149.61, 136.50, 131.86, 131.66, 129.78, 128.49, 126.87, 123.55, 121.95, 121.88, 119.19, 118.72.

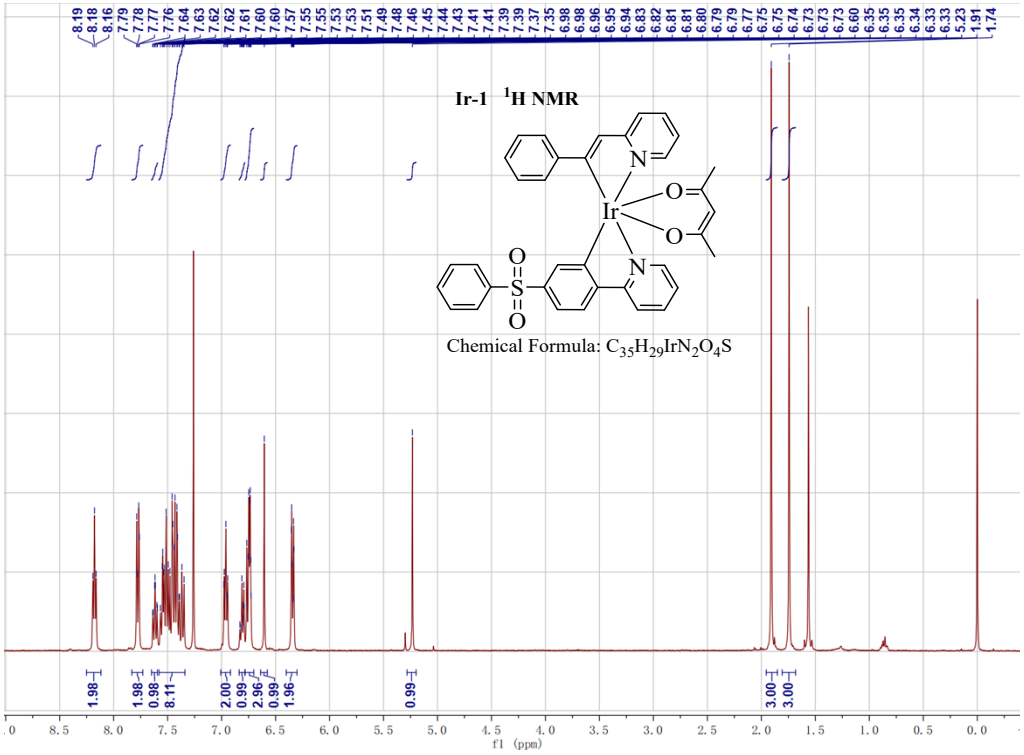
Ir-1 ^{1}H NMR
Chemical Formula: $C_{35}H_{29}IrN_2O_4S$
f1 (ppm)

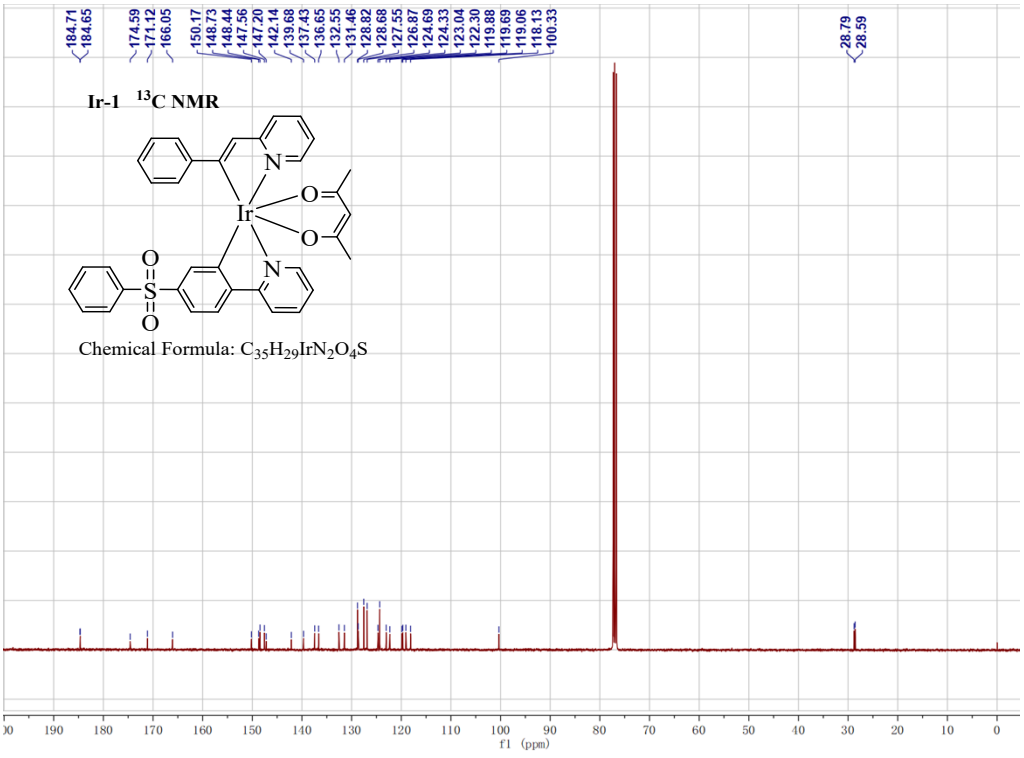
Ir-1 ^{13}C NMR
Chemical Formula: $C_{35}H_{29}IrN_2O_4S$
f1 (ppm)

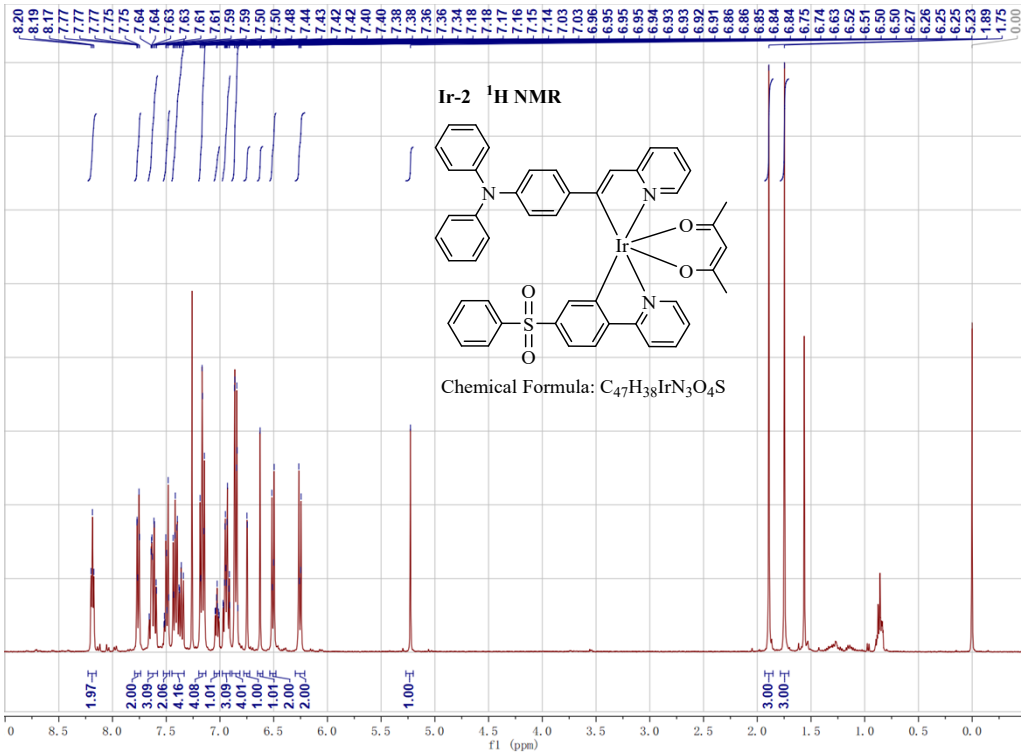
Ir-2 ^{1}H NMR
Chemical Formula: $C_{47}H_{38}IrN_3O_4S$
f1 (ppm)

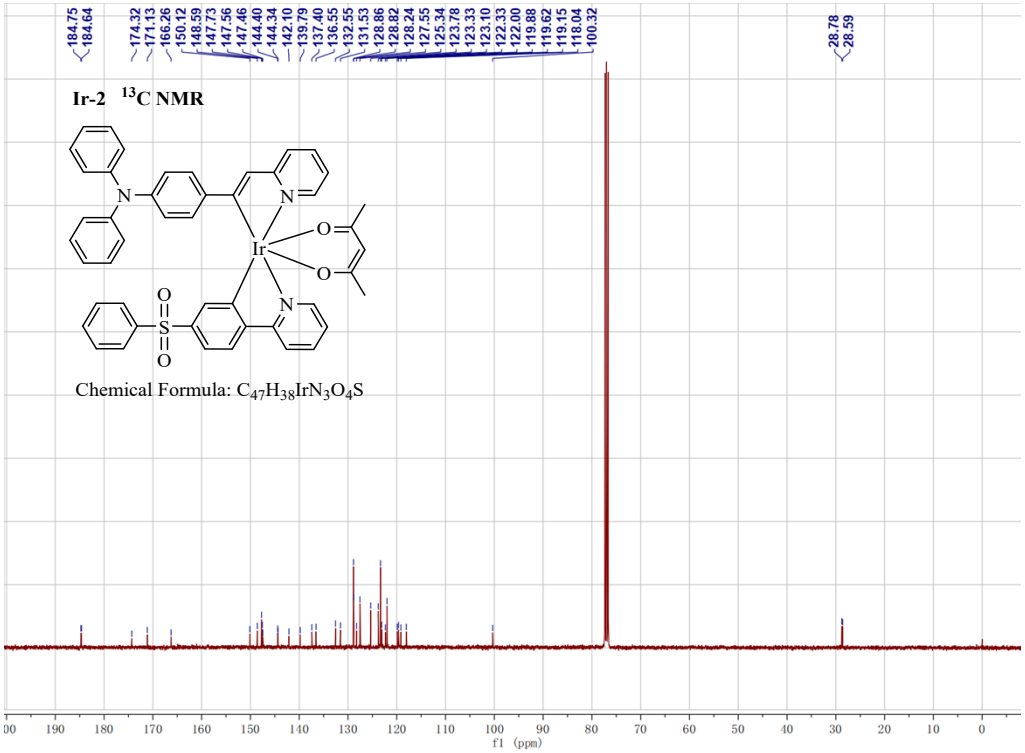
Ir-2 ^{13}C NMR
Chemical Formula: $C_{47}H_{38}IrN_3O_4S$
f1 (ppm)

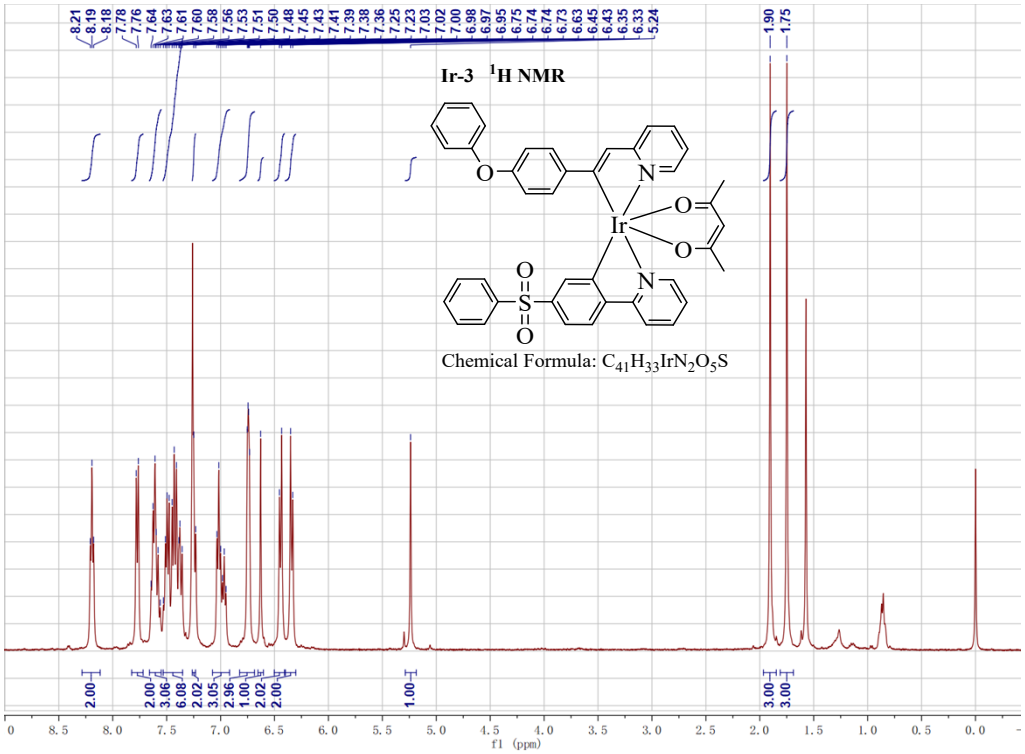

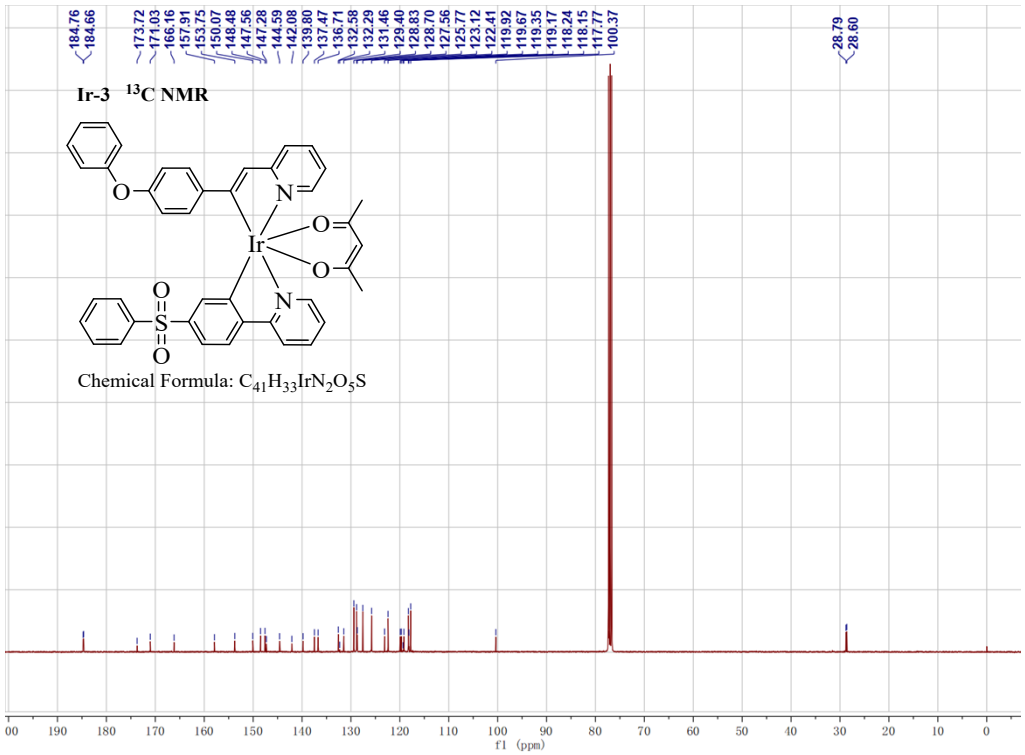

Fig. S1 NMR spectra of these unsymmetric Ir^{III}(ppy-vpy)acac-type complexes.

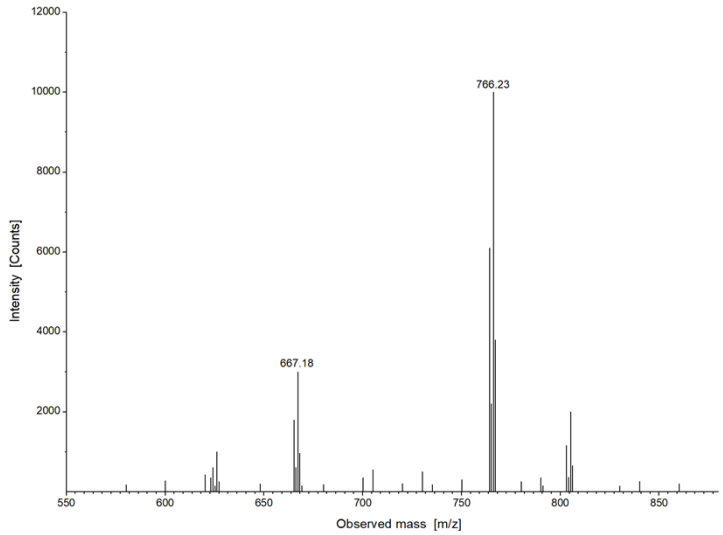

(a) Ir-1

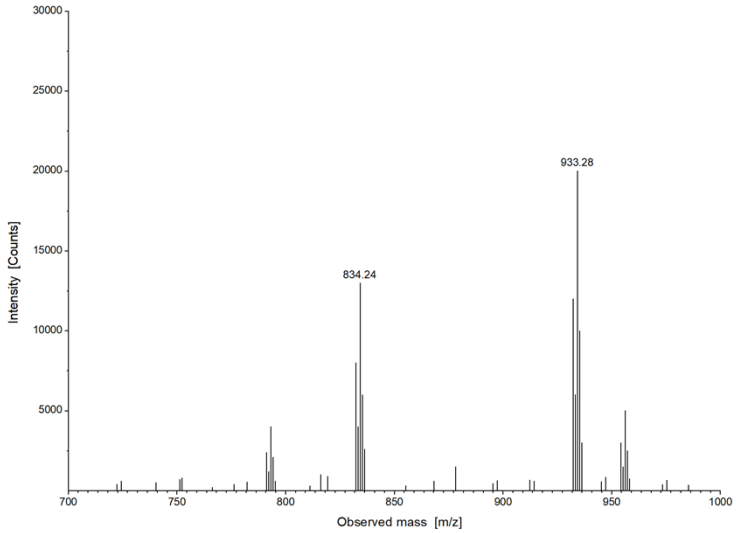

(b) Ir-2

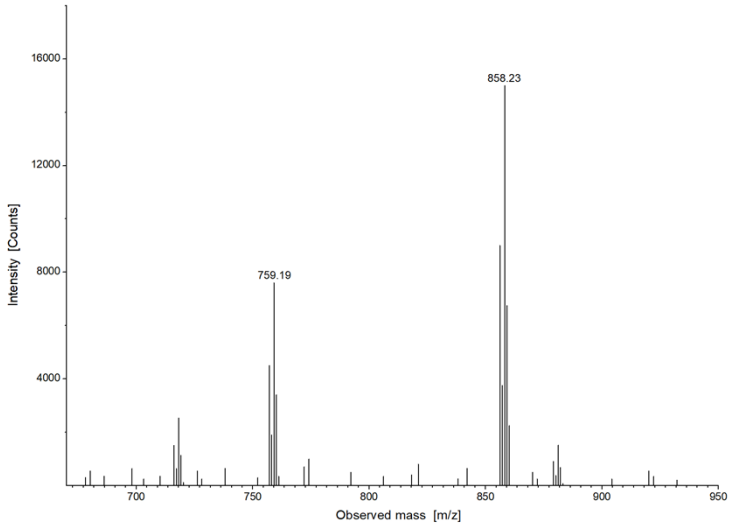

(c) Ir-3

Fig. S2 Mass spectra of these unsymmetric Ir^{III}(ppy-vpy)acac-type complexes.

Table S1 Crystal and data parameters for **Ir-1**.

compound	**Ir-1**
CCDC No.	2289776
Formula	$C_{35}H_{29}IrN_2O_4S$
Formula weight	765.86
Crystal system	Triclinic
Space group	$P\bar{1}$
a (Å)	10.118(3)
b (Å)	11.146(3)
c (Å)	15.176(5)
α (deg)	104.493(10)
β (deg)	93.639(10)
γ (deg)	112.115(10)
V (Å^3)	1511.3(8)
Z	2
D_{calcd} (g cm^{-3})	1.683
Crystal size (mm^3)	0.160×0.170×0.110
F (000)	756
μ (mm^{-1})	4.529
2θ range (deg)	4.13 - 54.986
Reflections collected	31672
Independent reflections	6908
Parameters	390
$R1$, $wR2$ [$I > 2.0\sigma$ (I)][a]	0.0198, 0.0437
$R1$, $wR2$ (all data)	0.0213, 0.0443
GOF on F^2 [b]	1.067

[a] $R1 = \Sigma||F_0|-|F_c||/\Sigma|F_0|$. $wR2 = \{\Sigma[w(F_0^2-F_c^2)^2]/\Sigma[w(F_0^2)^2]\}^{361/2}$.

[b] GOF = $[(\Sigma w|F_0|-|F_c|)^2/(N_{obs}-N_{param})]^{1/2}$.

Table S2 Selected structural parameters of **Ir-1**.

Bond angles (°)				Bond lengths (Å)	
O(1)-Ir(1)-O(2)	88.24(7)	C(16)-Ir(1)-C(29)	86.05(9)	Ir(1)-O(1)	2.1394(17)
N(1)-Ir(1)-O(1)	96.16(7)	C(29)-Ir(1)-O(1)	95.66(8)	Ir(1)-O(2)	2.1550(17)
N(1)-Ir(1)-O(2)	89.00(7)	C(29)-Ir(1)-O(2)	174.18(8)	Ir(1)-N(1)	2.0440(19)
N(2)-Ir(1)-O(1)	88.07(7)	C(29)-Ir(1)-N(1)	94.86(9)	Ir(1)-N(2)	2.034(2)
N(2)-Ir(1)-O(2)	96.22(7)	C(29)-Ir(1)-N(2)	79.64(9)	Ir(1)-C(16)	1.981(2)
N(2)-Ir(1)-N(1)	173.39(8)	O(3)-S(1)-C(14)	108.32(12)	Ir(1)-C(29)	1.987(2)
C(16)-Ir(1)-O(1)	176.30(8)	O(3)-S(1)-C(17)	107.60(13)	S(1)-O(3)	1.439(2)
C(16)-Ir(1)-O(2)	90.31(8)	O(4)-S(1)-O(3)	119.25(13)	S(1)-O(4)	1.4374(19)
C(16)-Ir(1)-N(1)	80.41(9)	O(4)-S(1)-C(14)	108.95(12)	S(1)-C(14)	1.767(2)
C(16)-Ir(1)-N(2)	95.48(9)	O(4)-S(1)-C(17)	108.28(12)	S(1)-C(17)	1.767(3)
C(17)-S(1)-C(14)	103.26(12)	C(6)-N(1)-C(10)	118.9(2)	O(1)-C(2)	1.268(3)
C(2)-O(1)-Ir(1)	125.11(17)	C(10)-N(1)-Ir(1)	115.79(15)	O(2)-C(4)	1.274(3)
C(4)-O(2)-Ir(1)	125.07(16)	C(31)-N(2)-Ir(1)	115.17(16)	N(1)-C(6)	1.351(3)
C(6)-N(1)-Ir(1)	125.12(16)	C(35)-N(2)-Ir(1)	125.14(17)	C(29)-C(30)	1.356(3)

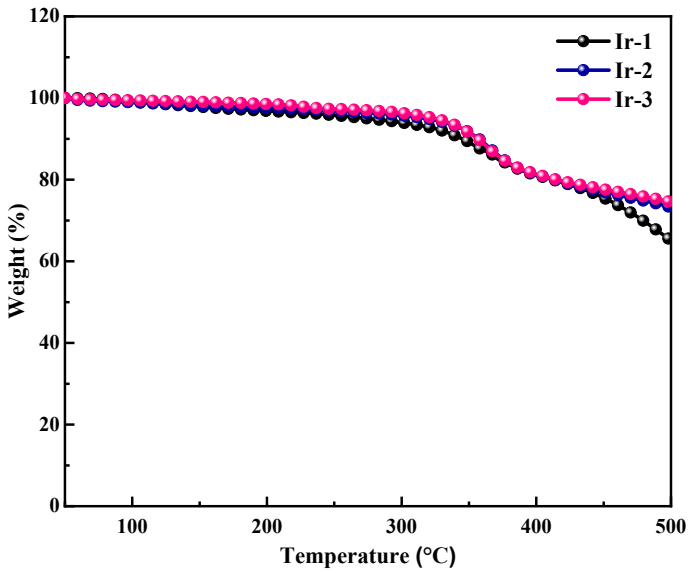

Fig. S3 TGA curves of these unsymmetric Ir^{III}(ppy-vpy)acac-type complexes.

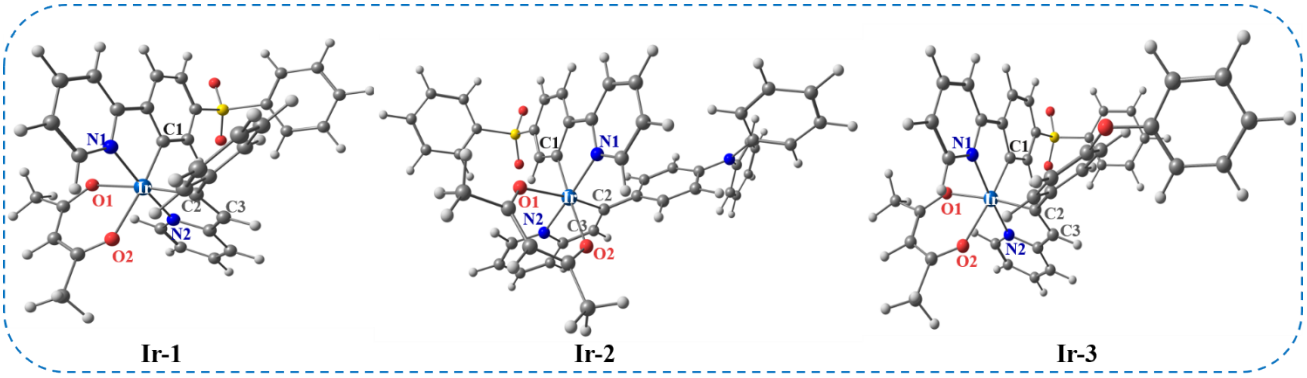

Fig. S4 Optimized S_0 geometries for **Ir-1**, **Ir-2** and **Ir-3**.

Table S3 Optimized S_0 geometries with key structural parameters for these Ir^{III}(ppy-vpy)acac-type complexes.

	Ir-1	**Ir-2**	**Ir-3**
Bond length (Å)			
Ir-O1	2.194	2.194	2.194
Ir-O2	2.196	2.200	2.195
Ir-N1	2.071	2.073	2.067
Ir-N2	2.067	2.068	2.073
Ir-C1	2.005	2.006	2.006
Ir-C2	2.009	2.012	2.010
C2-C3	1.365	1.367	1.366
Bond angle (°)			
N1-Ir-N2	176.110	175.917	176.037
N1-Ir-C1	80.320	80.301	80.308
N1-Ir-O1	86.822	86.813	86.621
O1-Ir-O2	86.461	86.380	86.472
O1-Ir-C2	173.738	173.844	173.700
O2-Ir-N2	89.768	89.865	89.912
O2-Ir-C1	173.868	174.142	173.970
N2-Ir-C2	79.937	80.000	79.941
C1-Ir-C2	91.800	90.805	91.323

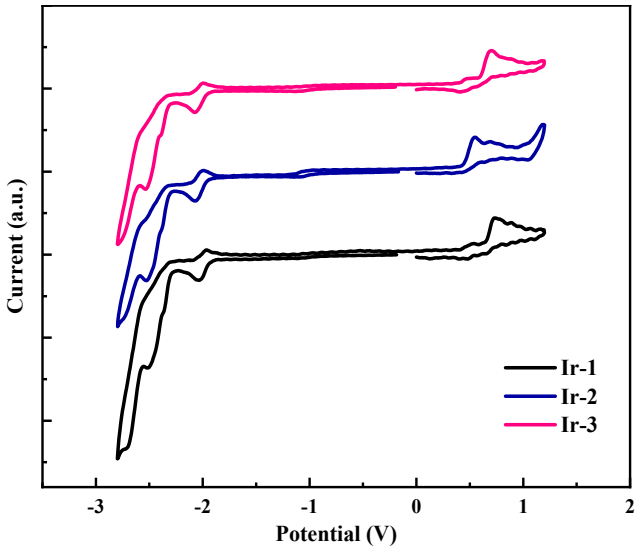

Fig. S5 Cyclic curves of these unsymmetric Ir^{III}(ppy-vpy)acac-type emitters are measured in degassed *N,N*-Dimethylformamide at room temperature.

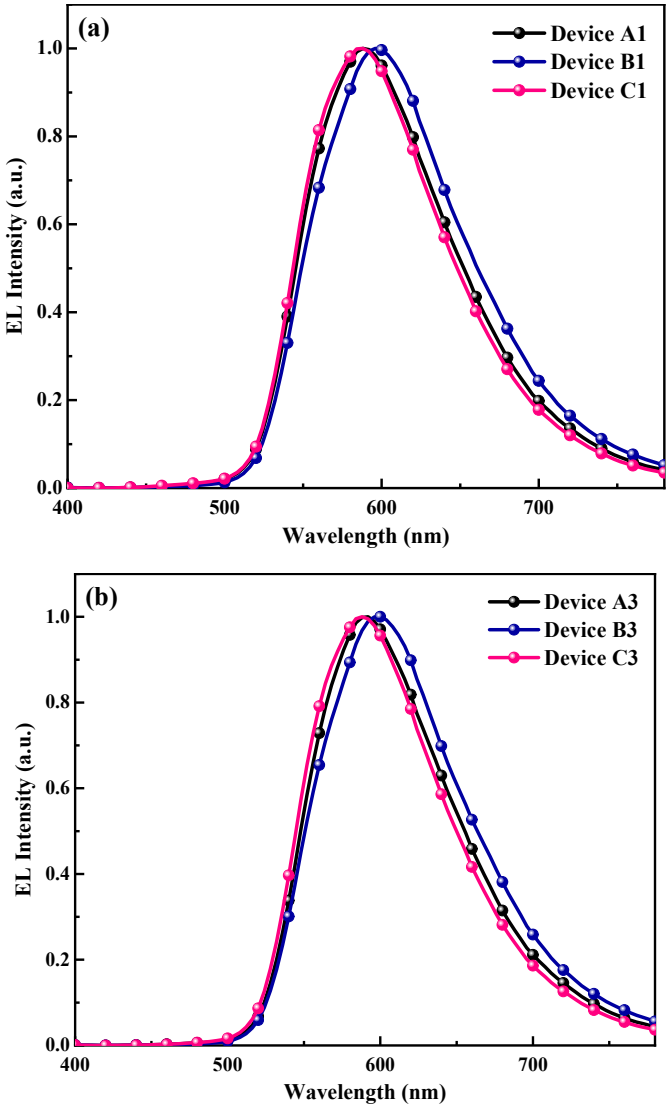

Fig. S6 EL spectra for devices **A1**, **A3**, **B1**, **B3**, **C1** and **C3** at *ca.* 9 V.

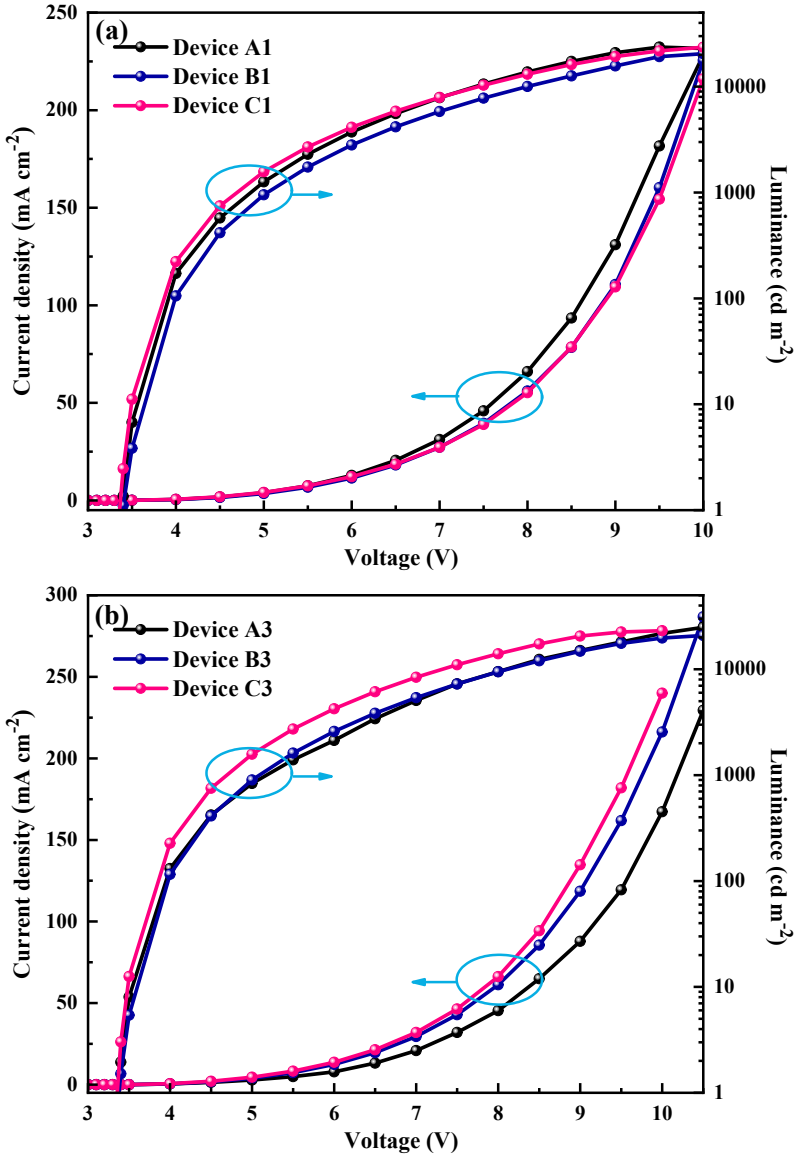

Fig. S7 Current-density–voltage–luminance (*J*-*V*-*L*) curves for devices of **A1**, **A3**, **B1**, **B3**, **C1** and **C3**.

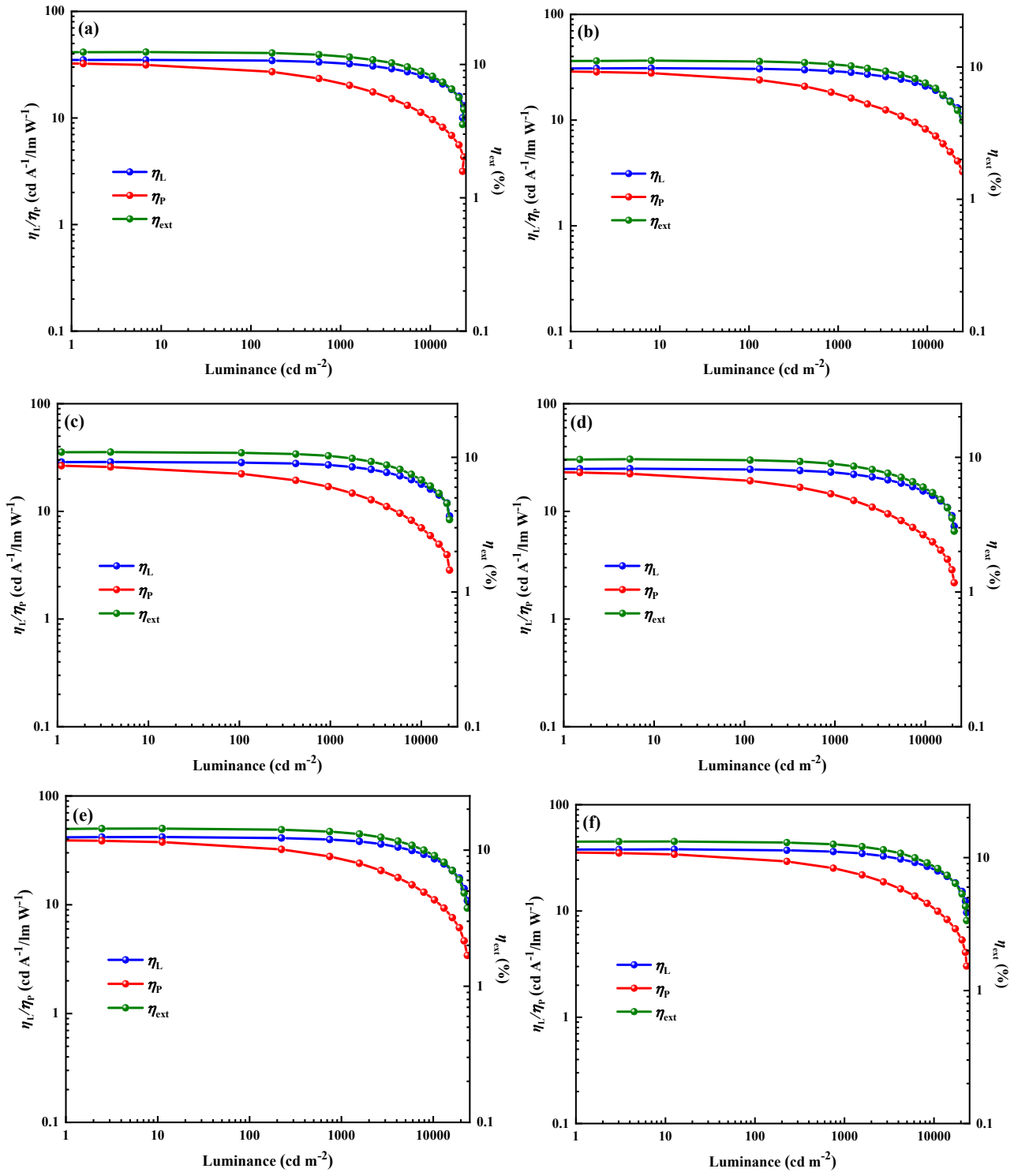

Fig. S8 Relationship between EL efficiencies and luminance for the optimized devices. (a) Device **A1**, (b) Device **A3** (c) Device **B1** (d) Device **B3**, (e) Device **C1** and (f) Device **C3**.